

Multi Response Optimization and Experimental Investigations into the Impact of Wire EDM on the Tribological Properties of Ti–6Al–4V

Basil Kuriachen¹ · K. P. Lijesh² · P. Kuppan³

Received: 24 June 2017 / Accepted: 30 December 2017 / Published online: 24 January 2018
© The Indian Institute of Metals - IIM 2018

Abstract Titanium (Ti) alloy, Ti–6Al–4V (commonly known as Ti64), is employed in numerous applications due to their superior strength to weight ratio, low cost to performance ratio, tensile strength, and corrosion resistance properties. However, due to its poor tribological (friction and wear) properties and difficult-to-machine material, its implementation in the intended applications is limited. Nevertheless, Ti64 can be accurately machined using wire electrical discharge machining (WEDM) and further, this process develops a recast layer on the surface of Ti64, which posses larger percentage of oxygen. Therefore, in the present work, it is hypothesized that, the presence of the recast layer on the surface of Ti64 may enhance its tribological properties. To validate the proposed hypothesis, pins of (1) pure Ti64 and (2) WEDMed Ti64 were slid against EN32 steel disc on a pin on disc experimental setup for load of 50 N, rotational speed of 200 rpm and sliding distance of 500 m. In-situ analysis (scanning electron microscope and energy dispersive spectroscopy) and mechanical properties (nano-hardness and elastic modulus) were performed on the pin's surface, to identify the change in properties. Obtained results indicated significant increase in the oxide layer formation, consequently enhanced the tribological properties of WEDMed Ti64 compared to pure Ti64. To understand the tribological

behavior of WEDMed Ti64 at other rotational speed and load, second set of experiments was performed by varying load (50, 70 and 90 N) and rotational speed of (200, 400 and 600 rpm). It was observed that wear values were not proportional to increase in load and speed. To identify the condition favoring the tribological behavior, multi-response optimization technique was performed and the identified load and speed values for the optimum tribological behavior were estimated.

Keywords WEDM process · Wear · COF · Recast layer

1 Introduction

Ti64, is the most extensively used Ti alloy in aerospace, marine, automobile, and bio medical applications, because of their high strength to weight ratio, low cost to performance ratio, bio-compatible ability and corrosion resistance properties. However, their application is limited due to their poor tribological properties (i.e. high wear and COF values) [1] and poor machinability (i.e. difficult to machine using conventional machining process) [2]. Nevertheless, the tribological properties of Ti64 can be improved by: (1) adding non-metallic and metallic elements to their surface, (2) artificial surface texturing processes, (3) achieving thin coating by iron implantations, magnetron sputtering, nitriding, boriding, deposition with laser ablation [3–7] and (4) surface oxidation [8], etc. However, first three surface modification techniques are uneconomical and therefore researchers also have focused their work in understanding the beneficial of formation of oxide layer on Ti64 for the improvement of tribological properties [9, 10]. To understand the wear behavior of Ti64, Mao et al. [8] performed dry sliding wear tests for Ti64 alloy under a load ranging

✉ Basil Kuriachen
basilkuriachen@gmail.com

¹ Department of Mechanical Engineering, National Institute of Technology Mizoram, Aizawl, India

² Department of Mechanical Engineering, National Institute of Technology Karnataka, Mangaluru, India

³ School of Mechanical and Building Sciences, VIT University, Vellore, Tamil Nadu, India

from 50 to 250 N at 25–500 °C. From their experiment, it was concluded that the wear rate increased linearly with increase in load for operating temperature 25–200 °C, while the wear rate decreased at higher temperature due to the existence of tribo-oxide layer. Jun et al. [10] studied the tribological characteristics of Ti64 alloy sliding against GCr15 under high speed (30–70 m/s), and applied pressure of: 0.25–1.5 MPa. They concluded that the formation of oxides TiO, TiO₂ and V₃O₄ at higher temperature, has resulted in enhanced tribological behavior. Li et al. [11] studied the wear behaviour of Ti64 alloy at sliding velocities of 0.5–4.0 m/s and they observed remarkable variation of wear rate as a function of velocity. With the fluctuation of wear rate, Ti64 alloy underwent the transitions of wear mechanisms from the combination of delamination wear and oxidative wear at lower speeds to delamination wear at 2.68 m/s, and then to oxidative wear at 4 m/s. The thickness of oxidative layer increased with increase in speed. These oxide layers played an essential role in protection of base material and in reducing the wear rate. From the above discussion it can be concluded that the oxide layer formed on the surface during high temperature experiments, acts as a protective layer for Ti64, which enhances the tribological behavior.

On the other hand, Ti64 comes under the category of difficult-to-machine materials due to its superior material and mechanical properties. Therefore, advanced and non-conventional manufacturing processes like (1) electrical discharge machining, (2) laser machining (3) abrasive water jet machining, etc. are required for machining them. Among these machining, wire electrical discharge machining (WEDM) is widely accepted machining process for hard and brittle materials (electrically conductive materials) due to their higher accurate machining and additionally any complex shapes can be achieved. WEDM works on the principle known as “localized melting and vaporization of electrode materials” where high thermal energy is generated through controlled discrete sparks between the tool electrode and work piece [11, 12]. One of the unique characteristics of WEDM process is that, during the machining operation, it develops a recast layer, which has higher content of oxides and the developed recast oxide layer formed may enhance the tribological properties [13]. In this regard, Bonny et al. [14] performed comparative dry reciprocating sliding experiments on samples of WC–Co hard metals with 6–12 wt% Co which was surface finished by grinding, polishing and wire-electro-discharge machining (WEDM). They concluded that, fine finishing by WEDM process played a vital role in enhancing the tribological properties of the material. Xu et al. [16] investigated the tribological behavior of WEDMed 7075Al alloys under dry sliding condition on a pin-on-disk wear tester. They concluded that the harder recast layer formed

on the surface of materials were significantly able to reduce the wear scar depth and enhance the durability of 7075 Al alloy. However deteriorating tribological behavior of WEDMed ZrO₂–TiN composites flats were observed by Bonny et al. [15]. Therefore it can be concluded that the recast layer formed during WEDM process can provide both deteriorating and enhancing tribological behaviour based on the surface finish and material. Further, as per author’s knowledge, no work have been reported on tribological studies of WEDMed Ti64. Therefore in the present work, the tribological behavior of WEDMed Ti64 material has been investigated. For this, pins made of pure Ti64 and WEDMed Ti64 were slid against EN32 steel disc using a POD test setup for load of 50 N, rotational speed 200 rpm and sliding distance of 500 m. The performance of the experiment was evaluated by measuring the wear depth and COF with sliding distance. Further, in-situ analysis using [scanning electron microscope (SEM) and energy dispersive spectroscopy (EDS)] and mechanical properties (nano-hardness and elastic modulus) were performed on the pin’s surface, to identify the change in properties. From SEM images, the wear morphology was envisaged while from EDS, qualitative value of elemental composition was obtained. From the obtained results, it was concluded that the recast layer was able to enhance the tribological performance of Ti64.

Further, to understand the tribological behavior of WEDMed Ti64 with respect to the POD parameters, experiments were performed on the POD machine for different loads (50, 70 and 90 N) and rotational speeds (200, 400 and 600 rpm). It was identified that the tribological behavior did not deteriorate proportionally to the sliding speed and load i.e. they did not follow the Archard’s equation. To identify for lower wear and COF values, optimization using multi-response optimization based on desirability function technique was performed. The identified models for the wear rate and co-efficient of friction for optimum tribological condition has been estimated and presented.

2 Experimental Details

Commercially available Ti64 in the cylindrical form having a diameter of 8 mm was procured and was machined to 6 mm diameter. The surfaces of the materials were machined using Ee2EECUT NXG CNC WEDM machine. The parameters used for WEDM process were: (1) peak current: 3 A, (2) pulse on time: 32 μs, (3) pulse off time: 6 μs and (4) wire feed: 99 m/min.

In the present work, the tribological characteristics of WEDMed Ti64 were evaluated under distinctive contact loads and sliding speed using a pin-on-disc test setup (as

shown in Fig. 1). The experiments were performed by sliding Ti64 pin against EN32 steel disk under dry operating conditions and for a sliding distance of 500 mm. As per ASTM G99 standards, for dry test conditions under ambient temperature and for pin diameter 6 mm, the test duration was limited to a total distance of 500 m. Therefore, the experiments were performed for sliding distance 500 m. The performances of the experiments were evaluated by measuring the online wear and COF values. The depth of wear was measured using the linear variable differential transformer (LVDT) and COF was measured using the load cell. First set of experiments on POD were performed for (1) pure and (2) WEDM'ed Ti64 pin at a load of 50 N and sliding speed of 200 RPM. Second set of experiments were performed for WEDM'ed Ti64 pin for different contact loads of 50, 70 and 90 N and sliding speeds of 200, 400 and 600 rpm.

3 Results and Discussion

To understand and compare the change in surface properties due to the formation of recast layer, in situ analysis of the pure Ti64 and WEDMed Ti64 pin's surfaces have been carried out using scanning electron microscope (SEM) and energy dispersive spectroscopy (EDS). Obtained SEM and EDS images of pure Ti64 and WEDMed Ti64 pins are presented in Figs. 2 and 3 respectively. In Table 1, the exact percentage of different elements on the pin's surface is tabulated. From this table, it can be observed that the percentage of oxygen has increased from 3.61 to 23.22% by WEDM process.

Further change in mechanical properties due to recast layer have been studied using nano-indenter test setup. By maintaining constant loading and unloading rate of 1 mN/s, the hardness and elastic modulus values of the Ti64 pins have been determined from load–displacement curves using Oliver–Pharr method. Measured nano-hardness and

elastic modulus of both pins are shown in Figs. 4 and 5 respectively. From these figures, it can be observed that, both mechanical properties: nano-hardness and elastic modulus increase due to recast layer formation. From the above discussions it can be concluded that by recast process, both mechanical as well as oxygen percentage on the pin's surface have enhanced, which may result in providing enhanced tribological properties.

To understand the effect of recast layer on the tribological behavior such as wear and the COF values, experiments have been performed on the pin on disc test setup in dry-ambient condition for 50 N load, 200 rpm rotational speed and 500 m sliding distance. Measured COF and wear depth values for pure Ti64 and WEDMed pins for sliding distance of 500 m has been plotted in Figs. 6 and 7 respectively. From these figures, it can be observed that the COF and wear of depth values has reduced by 25 and 77% respectively by the formation of recast layer. Therefore it can be concluded that the tribological performance can be enhanced by forming recast layer through WEDM process and this validates the proposed hypothesis.

To understand the variation in tribological behavior of WEDMed Ti64 with load and sliding speed, number of experiments have been performed by varying the load (50, 70, 90 N) and sliding speed (200, 400, 600 rpm) for a sliding distance of 500 m. After performing the nine experiments, the obtained wear with sliding distance for three different selected cases (1) case 1: low wear (70 N, 400 rpm), (2) case 2: medium wear (70 N, 200 rpm) and (3) case 3: high wear (90 N, 600 rpm) is plotted in Fig. 8. From this figure, occurrence of both transient and steady state wears are observed and the transition of transient wear to steady state wear occur after 100 m sliding distance. However, the magnitude of transient wear and slope of steady state wear is observed to be different for different cases.

Acquired final wear rate and COF values are tabulated in Table 2. From this table, it can be concluded that the wear rate and COF are not proportionally increasing with load and sliding speed. Wear rate and COF values are found to be minimum for 70 N load and 400 rpm and maximum for 90 N load and 600 rpm.

To understand the reason for different tribological behaviour at different load and speed, in situ analysis using SEM and EDS have been performed on Ti64 pins, for the selected three cases (1) case 1: low wear (70 N, 400 rpm), (2) case 2: medium wear (70 N, 200 rpm) and (3) case 3: high wear (90 N, 600 rpm). Acquired SEM images for aforementioned three cases are presented in Fig. 9. As depicted from Fig. 9a, b, for case 1 and case 2, a mixture of black and white color is observed on the pin's surface, While in case of case 3, majority of the surface is covered

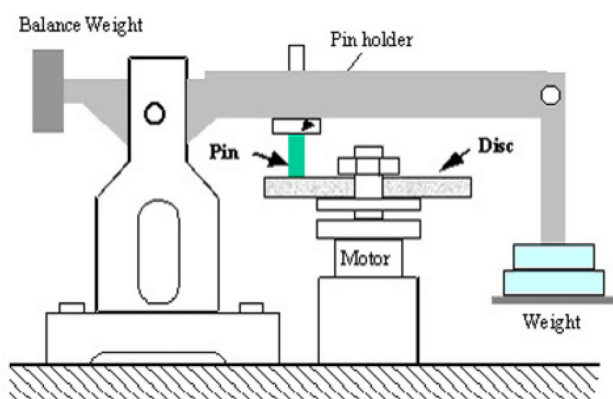


Fig. 1 Schematic representation of pin-on-disc tribometer

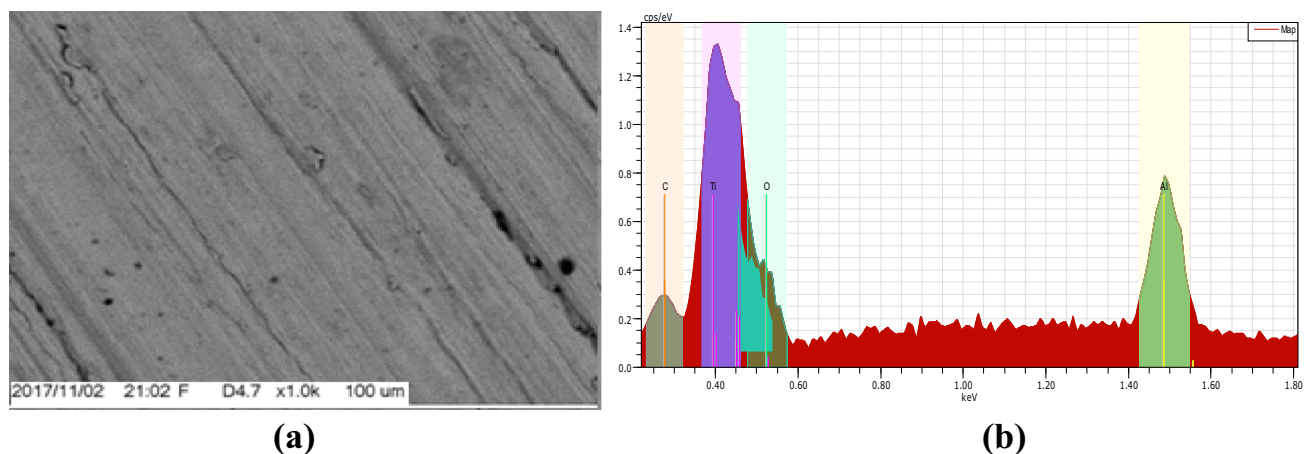


Fig. 2 SEM and EDS image of pure Ti64 pin. **a** SEM image, **b** EDS image

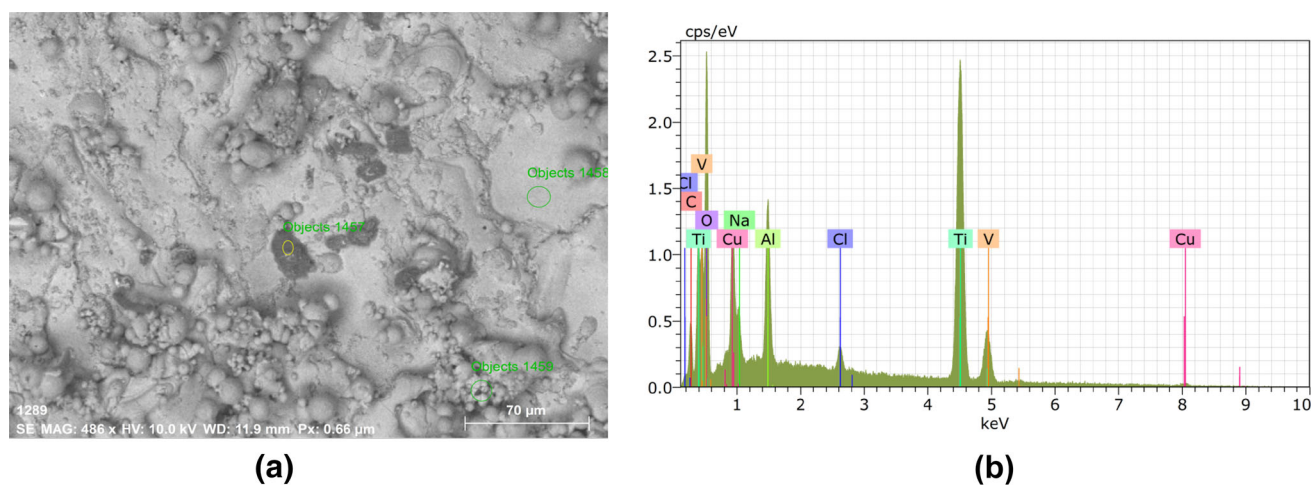


Fig. 3 SEM and EDS image of WEDMed pin. **a** SEM image, **b** EDS image

with white colored layer and with severe deformation, as observed from Fig. 9c.

Zoomed SEM images shown in Fig. 10 have been used to understand the wear morphology for different cases. For case 1 (from Fig. 10a), only abrasive wear is observed on the pin's surface, however for case 2 (from Fig. 10b), along with abrasive wear, some plastic deformation is also observed. In case of case 3, majority of the pin's surface is observed with plastic deformation, from Fig. 10c.

Now, to identify the reason for the different wear morphology and different layer colors, compositions of elements are estimated at two different location of case 1 pin's surface (as shown in Fig. 11) using EDS. Obtained elemental compositions for two locations are tabulated in Table 3. From this table and Fig. 11, it can be concluded that, presence of oxygen at white colored layer is minimal while at black colored layer, presence of oxygen is high. Therefore, it can be concluded that, the presence of oxide layer in case 1 has provided a protection layer and resulted

Table 1 Percentage composition of elements of pure and WEDMed Ti64 pins

Element	Pure Ti64 (%)	WEDMed Ti64 (%)
Ti	88.48	61.73
Al	6.58	3.96
O	3.32	23.51
C	1.54	2.53

in reduced wear, while the absence of oxide-protective layer for case 3 has resulted in plastic deformation and resulted in high wear.

4 Regression Modeling and Optimization

In the following section, the load and speed corresponding to the optimum wear rate and COF values are identified by using commercially available Design Expert software

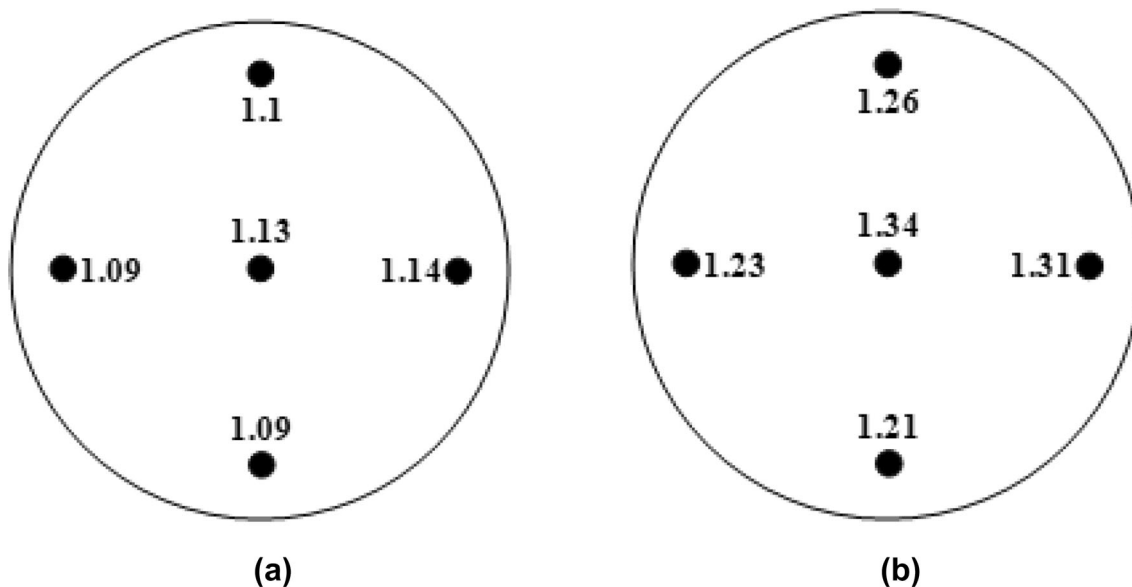


Fig. 4 Measured nano-hardness (GPa) of pure Ti64 and WEDMed Ti64 pins. a Pure Ti64 pins, b WEDMed Ti64 pins

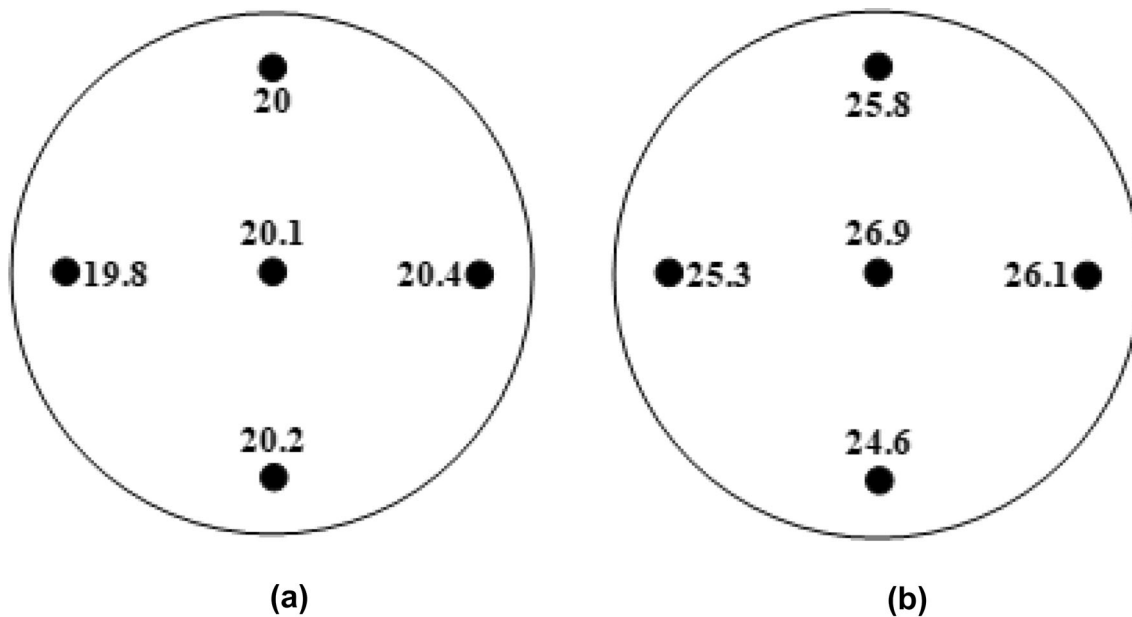


Fig. 5 Measured elastic modulus (GPa) of pure Ti64 and WEDMed Ti64 pins. a Pure Ti64 pins, b WEDMed Ti64 pins

package. The results obtained from the software are tabulated in Table 3 and the values have been analyzed statistically to obtain the optimum condition.

4.1 ANOVA for Wear Rate

Table 4 shows the effect of individual and interaction effect on the wear rate for second order quadratic model. The model is developed at 95% confidence level i.e., the factors with *p* value less than 0.05 are the significant factors. By analysing the *F*-value and *p* value, it is

understood that both the disc rotational speed and the applied load along with its quadratic terms are found to be significant (*A*, *B*, *A*², and *B*²). The *R*² value of 0.9853, Adj *R*² of 0.9706, Pred *R*² of 0.9255 and Adeq Precision of 23.374 show the dependency of the model. The Pred *R*² and Adj *R*² are in reasonable agreement with a difference of 0.1. Further, from the normal plot of residuals (Fig. 12a), it is inferred that the errors are normally distributed as the residuals falls on the straight line. The residual versus predicted (Fig. 12b) and residual versus run order (Fig. 12c) does not show any specific pattern and it is

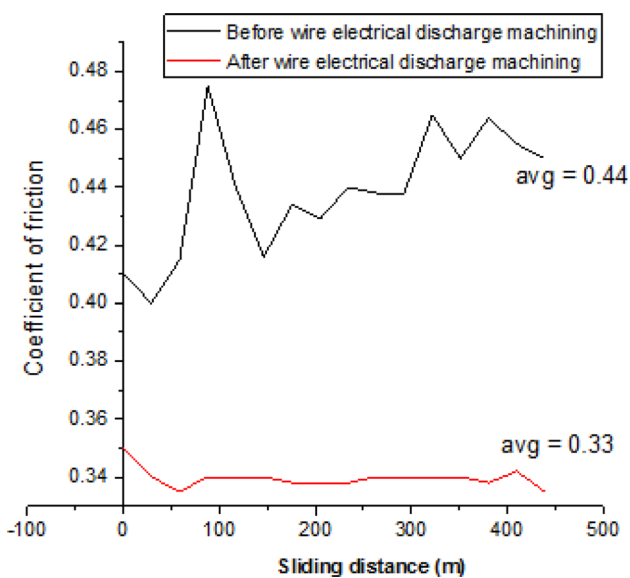


Fig. 6 Comparison of co-efficient of friction before and after WEDM of Ti-6Al-4V

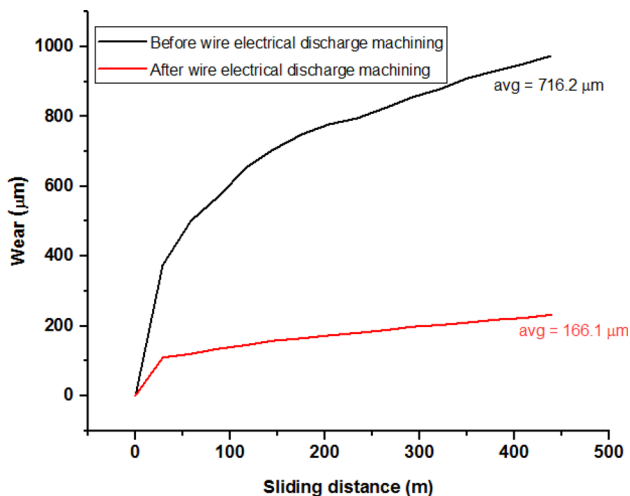


Fig. 7 Comparison of wear depth before and after WEDM of Ti-6Al-4V

structureless. Therefore, there is no reason to suspect any violation of independence or constant variance assumption. Therefore the developed model can be used to navigate in the design space.

4.2 ANOVA for COF

The analysis of variance for COF is tabulated in Table 5. In this table, the values with high F-value and *p* value less than 0.05 have been identified as the important parameters, which influences the co-efficient of friction values. The main factors considered for the optimization such as disc: rotational speed, load and their interactions as well as the quadratic term are found to be significant. The R-squared,

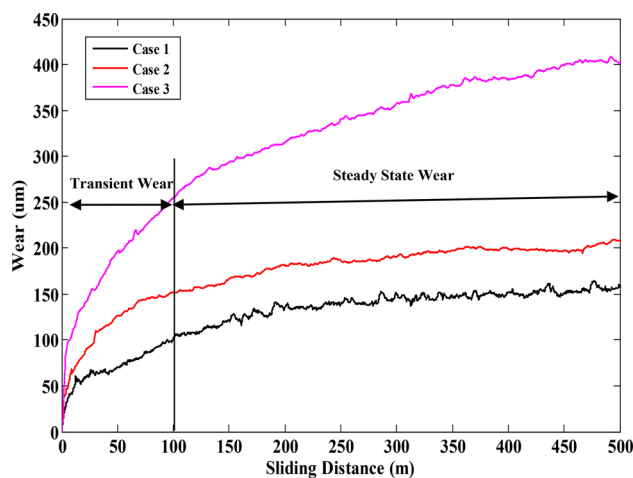


Fig. 8 Wear behavior for three different cases

Adj-R-Squared, Pred R-Squared, Adeq Precision are found to be 0.9979, 0.9944, 0.9752 and 50.456 respectively during the residual analysis. Moreover, the “Pred-R-Squared” of 0.9752 is in reasonable agreement with the “Adj-R-Squared” of 0.9944 with a difference less than 0.2. The normal probability plot, residual versus Predicted and residual versus run order have also been analyzed and plotted in Fig. 13a–c respectively. From these plots, the utilized model is found to be satisfactory.

4.3 Development of Regression Models

In this section, the wear rate and co-efficient of friction have been modeled in terms of the pin-on-disc parameters using multiple regression analysis and the dependency of the developed models have been tested. All variations of the models (linear, interaction, quadratic, and cubic) have been analyzed and the best fit model is selected. The developed models for the wear rate and co-efficient of friction are given in Eqs. (1) and (2) respectively.

$$W = 3.78 \times 10^{-4} - 3.54 \times 10^{-7}N - 6.723 \times 10^{-6}L + 5.58 \times 10^{-10}N^2 + 5.15 \times 10^{-8}L^2 \tag{1}$$

$$COF = 0.831 - 6.86 \times 10^{-4}N - 0.013L + 1.13 \times 10^{-6}NL + 9.46 \times 10^{-7}N^2 + 8.96 \times 10^{-7}L^2 \tag{2}$$

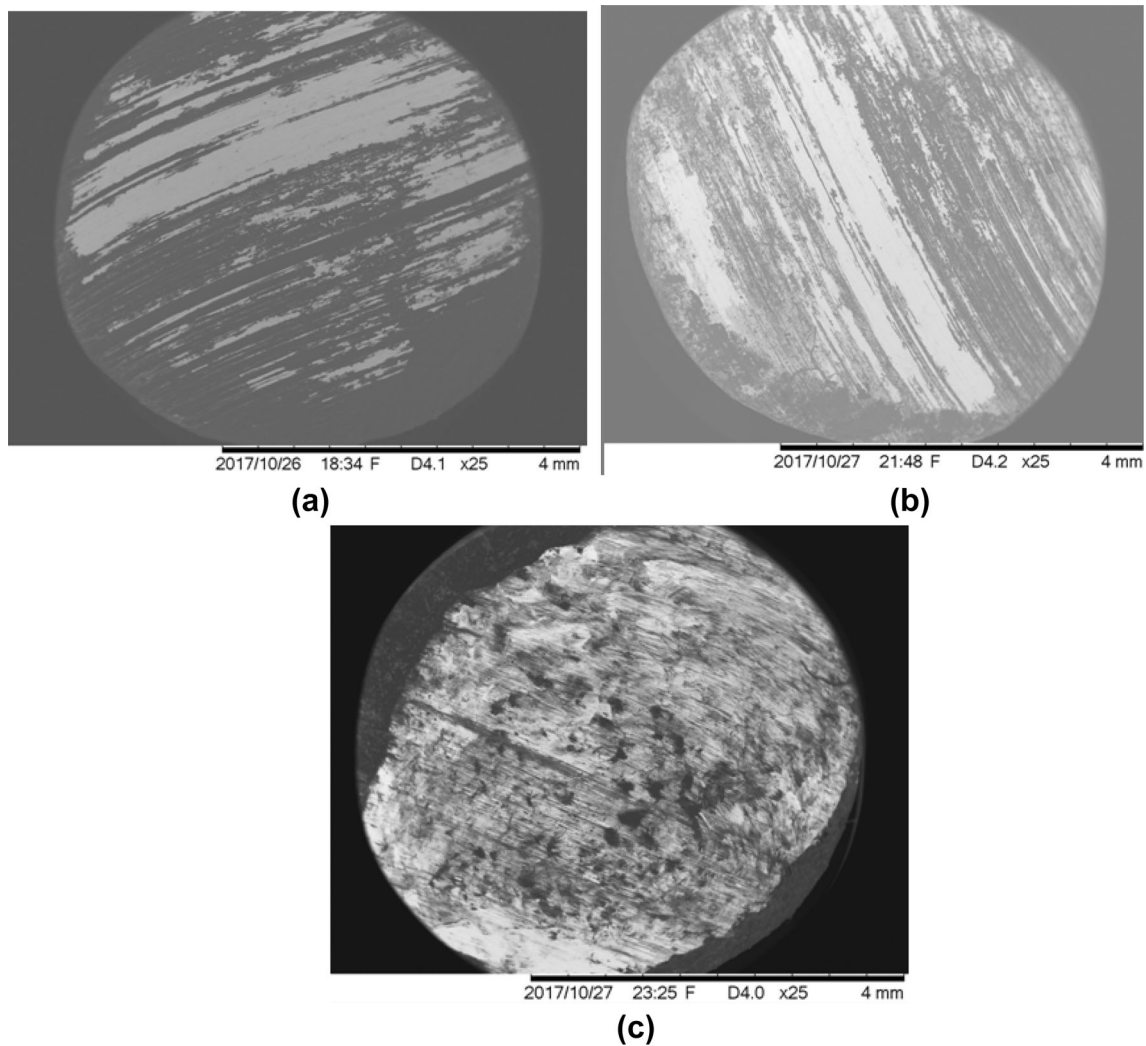
In the above equations, *W* is the wear rate, *COF* is the coefficient of friction, *L* is the load and *N* is the rpm

4.4 Multi-response Optimization of the Processes Parameters

The optimum pin-on-disc parameter combination is needed to conduct the experimental investigations into the effect of WEDM parameters on the tribological behavior. Hence, the

Table 2 Experimental design and output response

Sl. no	Disk rotation speed rpm	Force (N)	Wear rate $\times 10^{-4}$ (mm ³ /Nm)	COF
1	200	50	1.2008	0.337
2	200	70	1.1432	0.299
3	200	90	1.4237	0.342
4	400	50	1.1668	0.322
5	400	70	1.0989	0.295
6	400	90	1.3871	0.337
7	600	50	1.6484	0.385
8	600	70	1.4458	0.364
9	600	90	1.7842	0.408

**Fig. 9** SEM images of the pins surface. **a** Case 1, **b** case 2, **c** case 3

optimum parameters are obtained by applying the multi-response optimization technique developed by Derringer and Suich [17] i.e., desirability functions, which is applied in various manufacturing process for optimization [18–20].

The desirability function approach is one of the most widely used methods in industry for optimization of multi response process. It have been originally developed by Harrington and thereafter modified by Derringer and Suich

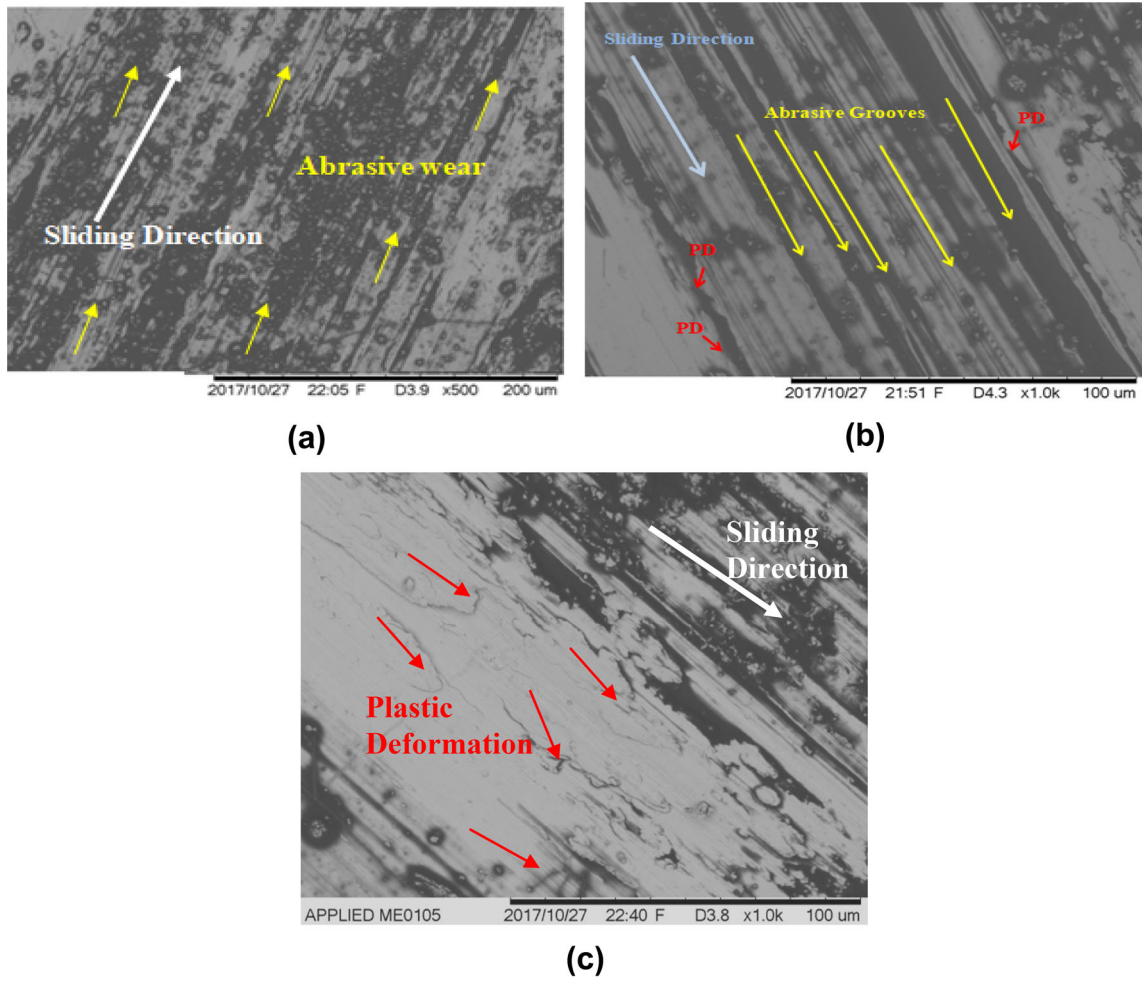


Fig. 10 SEM images of the pin’s surface. a Case 1, b case 2, c case 3

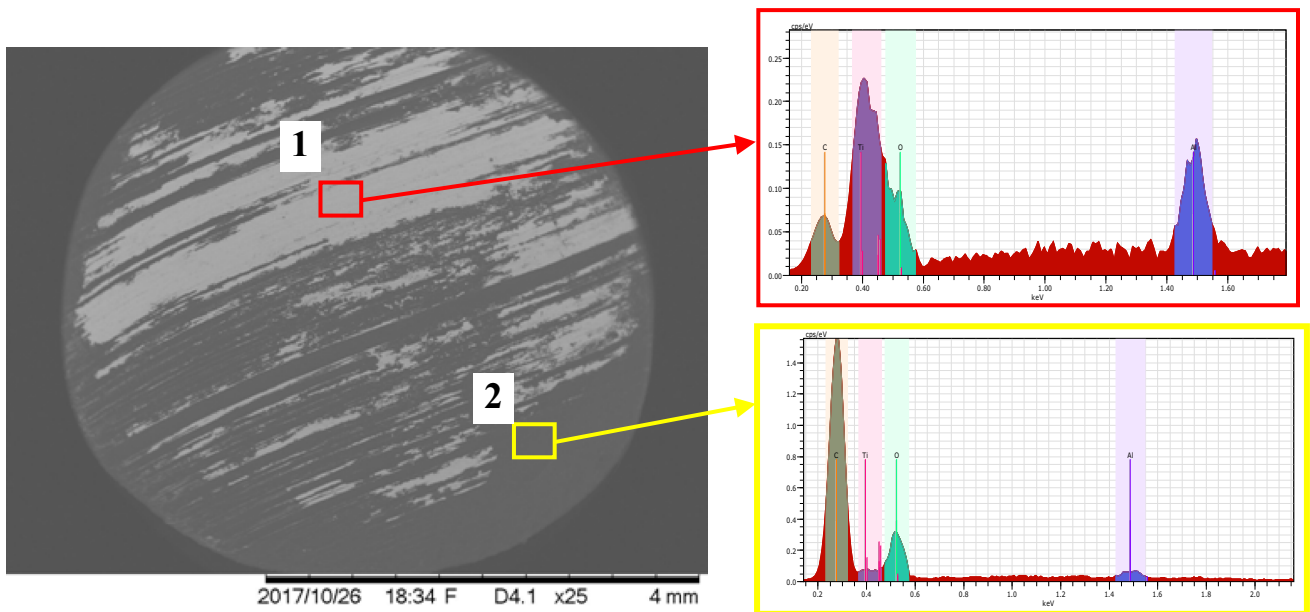


Fig. 11 SEM and EDAX images for case 2 pin’s surface

Table 3 Percentage composition of elements of pure and WEDMed Ti64 pins

Element	1	2
Ti	85.07	46.55
Al	7.43	31.45
O	5.49	19.92
C	2.01	2.08

[17]. The basic idea of this approach is to transform a multi-response problem into a single response problem by mean of mathematical transformations. The desirability function $d_i(Y_i)$ assigns a number between 0 and 1 to the possible values for each response ($Y_i(x)$), $d_i(Y_i) = 0$ for completely undesirable value and $d_i(Y_i) = 1$ for completely desirable or ideal response value. Once this function is defined for each of the response of interest, an overall objective function (total desirability) is defined as the geometric mean of the individual’s desirability.

$$D = (d_1(Y_1)d_2(Y_2) \dots d_n(Y_n))^{-1/n} \tag{3}$$

Here ‘n’ denotes the number of responses. Depending on whether a particular response, Y_i has to be maximized, minimized or assigned a target value, a different desirability function $d_i(Y_i)$ can be used and they are proposed by Derringer and Suich [17]. Let L_i , U_i and T_i be the lower, upper and target values respectively, that are desired for response Y_i with $L_i \leq T_i \leq U_i$. If the response is of the “target is best” kind, then its individual desirability function is

$$d_i(Y_i) = \begin{cases} 0 & \text{if } Y_i(x) < L \\ \left(\frac{\hat{Y}_i(x) - L_i}{T_i - L_i}\right)^s & \text{if } L_i \leq Y_i(x) \leq T_i \\ \left(\frac{\hat{Y}_i(x) - U_i}{T_i - U_i}\right)^t & \text{if } T_i \leq Y_i(x) \leq U_i \\ 0 & \text{if } Y_i(x) > U \end{cases} \tag{4}$$

If a response is to be maximized, the individual desirability is defined as,

Table 4 ANOVA for wear rate

Source	Sum of squares	df	Mean square	F-value	p value Prob > F
Model	4.46E-09	4	1.12E-09	66.97	0.000643
A-disk rotational speed	2.06E-09	1	2.06E-09	123.48	0.000373
B-load	5.59E-10	1	5.59E-10	33.55	0.004414
A ²	9.98E-10	1	9.98E-10	59.95	0.001498
B ²	8.48E-10	1	8.48E-10	50.91	0.002041
Residual	6.66E-11	4	1.67E-11		
Cor total	4.53E-09	8			

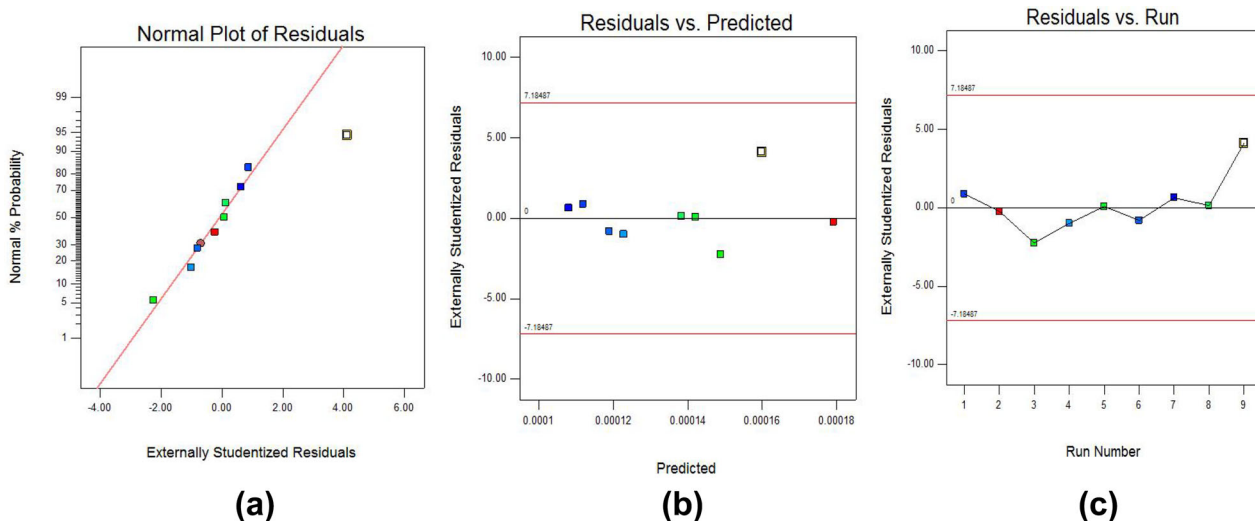


Fig. 12 Optimization of wear rate the pin-on-disc parameters. **a** Normal residuals plot, **b** residuals versus predicted wear, **c** residuals versus run order

Table 5 ANOVA table for coefficient of friction

Source	Sum of squares	df	Mean square	F-value	p value Prob > F
A-disk rotational speed	0.00534	1	0.00534	683.33	0.000123
B-load	0.000308	1	0.000308	39.43	0.008154
AB	8.1E−05	1	8.1E−05	10.36	0.048604
A ²	0.002863	1	0.002863	366.31	0.000311
B ²	0.002568	1	0.002568	328.61	0.000366
Residual	2.34E−05	3	7.81E−06		

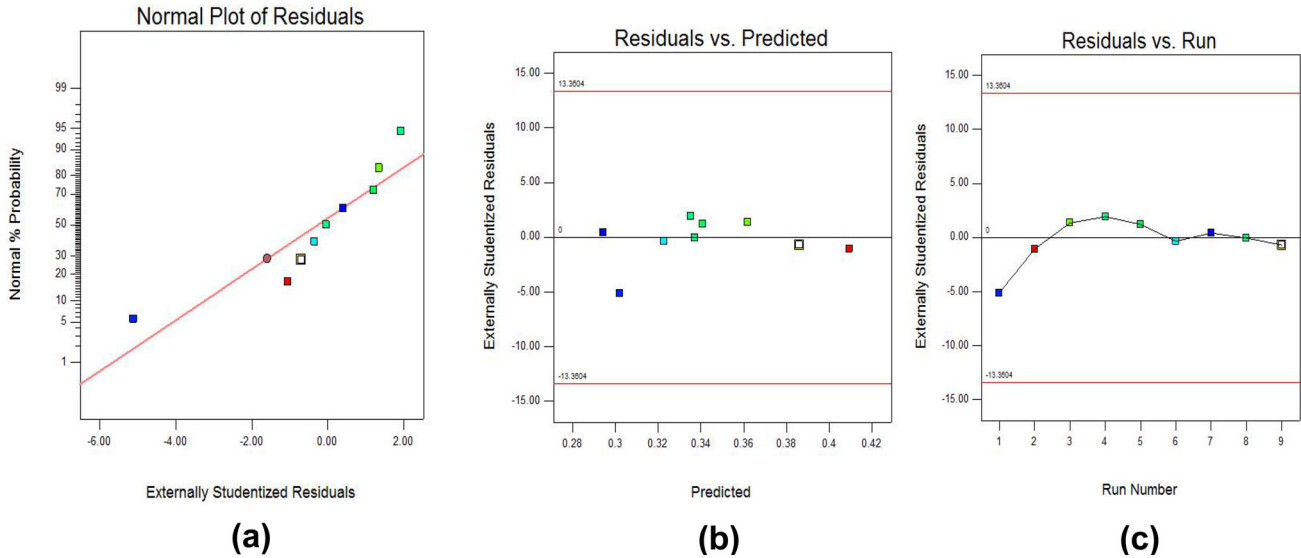


Fig. 13 Optimization of wear rate the pin-on-disc parameters. **a** Normal plot, **b** residuals versus predicted wear rate, **c** residuals versus run order

$$d_i(Y_i) = \left\{ \begin{array}{ll} 0 & \text{if } Y_i(x) < L \\ \left(\frac{\hat{Y}_i(x) - L_i}{T_i - L_i} \right)^s & \text{if } L_i \leq Y_i(x) \leq T_i \\ 1.0 & \text{if } Y_i(x) > T_i \end{array} \right\} \quad (5)$$

If the response is to be minimized, the individual desirability is

$$d_i(Y_i) = \left\{ \begin{array}{ll} 1.0 & \text{if } Y_i(x) < L \\ \left(\frac{\hat{Y}_i(x) - U_i}{T_i - U_i} \right)^s & \text{if } L_i \leq Y_i(x) \leq T \\ 0 & \text{if } Y_i(x) > U_i \end{array} \right\} \quad (6)$$

Implementation of desirability function based multi response optimization involves the following steps.

1. Conduct the experiments and fit response models for all the responses.
2. Obtain the individual desirability ($d_i(Y_i)$) for all the responses.
3. Combine the individual desirability to obtain the combined desirability (D).

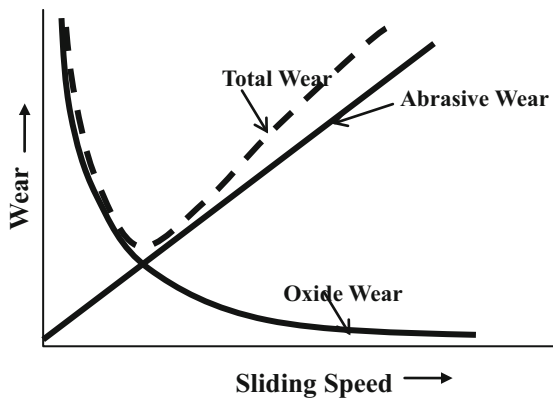
4. Maximize the combined desirability and identify the optimal process parameter settings.

The optimization of the pin-on-disc parameter based on the minimization criteria has been carried out (i.e., in order to achieve the minimum wear rate and minimum co-efficient of friction). The optimized tribometer parameters, response and achieved desirability are tabulated in the Table 6 and they can be used to perform the future tribological studies of WEDM samples.

The reason for the optimum tribological behavior may be due to the combined effect of abrasive wear and oxide wear, as shown in Fig. 14. Oxide wear is proportional to the contact area and inversely proportional to speed and contact temperature. While, abrasive wear is proportional to load, speed and indirectly proportional to the hardness of the material. As it can be observed that the oxide wear is inversely proportional to speed while abrasive wear is directly proportional to speed. Therefore, there exists an optimum location where the wear will be minimum.

Table 6 Optimized pin-on-disc parameters

Disc rotation speed (rpm)	Load (N)	Wear rate (mm ³ /Nm)	Coefficient of friction	Desirability
248	71	0.00011	0.294	1

**Fig. 14** Variation of wear with sliding speed

However to prove this, extensive Ex-situ analysis is required which will be performed in the future work.

5 Conclusion

In the present work, tribological studies were performed on (1) WEDM treated and (2) pure Ti64 material. In-situ analysis using SEM and EDS on both the pins confirmed the presence of recast layer possessing > 23% oxygen. It was hypothesized that the presence of oxygen on the surface enhanced the tribological behavior of Ti64. To validate the proposed hypothesis, experiments were performed on POD experimental setup, considering two types of pins (1) WEDMed pin and (2) pure Ti64. Pins were slid against EN32 steel disc for 50 N load, 200 rpm and 500 m sliding distance. It was observed that the COF and wear depth values were reduced by 25 and 77% respectively for WEDMed pin. Therefore, it was concluded that the formation of recast layer on the Ti64 pin due to WEDM process, has enhanced the tribological properties of Ti64.

In the second set of experiments, the tribological behavior of WEDMed Ti64 pin was studied by varying the load (50, 70 and 90 N) and speed (200, 400 and 600 rpm). From the experiments it was concluded that the wear rate did not follow the Archards equation, i.e. wear rate was not proportional speed and load. In addition, the operating condition (i.e. load and speed) providing favorable tribological behavior was determined using desirability function

approach technique. From the optimization technique, it was observed that the wear and COF were minimum for load of 71 N and 248 rpm respectively. This optimized parameters of Pin on Disc could be utilized to evaluate the maximum wear resistant and COF of WEDMed surfaces. The authors are in the process of investigating the effect of WEDM parameters on wear rate and COF.

Acknowledgement This work was supported by grants received from the Science and Engineering Research Board (SERB), DST, Govt. of India (Project ref. No. ECR/2016/001929). The authors gratefully acknowledge Mr. Siva, VIT University Vellore for the support provided to conduct the required experiments.

References

- Budinski K G, *Wear* **151** (1991) 203.
- Kuriachen B, Somashekhar K P, and Mathew J, *Int J Adv Manuf Technol* **76** (2015) 91.
- Yildiz F, Yetim A F, Alsaran A, and Efeoglu I, *Wear*, **267** 695.
- Wang S, Liao Z, Liu Y, and Liu W, *Surf Coat Technol* **252** (2014) 64.
- Mu M, Liang J, Zhou X, and Xiao Q, *Surf Coat Technol* **214** (2013) 124.
- Xiong D, Yang Y, and Deng Y, *Surf Coat Technol* **228** (2013) S442.
- Atar E, Kayali E S, and Cimenoglu H, *Surf Coat Technol* **202** (2008) 4583.
- Mao Y S, Wang L, Chen K M, Wang S Q, and Cui X H, *Wear* **297** (2013) 1032.
- Yerokhin A L, Nie X, Leyland A, and Matthews A, *Surf Coat Technol* **130** (2000) 195.
- Qu J, Blau P J, Watkins T R, Cavin O B, and Kulkarni N S, *Wear* **258** (2005) 1348.
- Li X X, Zhou Y, Ji X L, Li Y, and Wang S Q, *Tribol Int* **91** (2015) 228.
- Shichun D, Dongbo C, Zhenlong W, Guanxin W, and Yuan L, *Int J Mach Tool Manuf* **49** (2009) 788.
- Cheng D, Shi G, Shi G, Xu Z, and Zhu K, *Micro Nano Lett* **12** (2017) 209.
- Bonny K, De Baets P, Quintelier J, Vleugels J, Jiang D, Van der Biest O, and Liu W, *Tribol Int* **43** (2010) 40.
- Bonny K, De Baets P, Vleugels J, Salehi A, Van der Biest O, Lauwers B, and Liu W, *Wear* **265** (2008) 1884.
- Xu J, Qiu R, Xia K, Wang Z, Xu L, and Yu H, Study on mild and severe wear of 7075 aluminum alloys by high-speed wire electrical discharge machining. In Seventh International Conference on Electronics and Information Engineering (Vol. 10322, p. 103224B). International Society for Optics and Photonics (2017).
- Derringer G, and Suich R, *J Qual Technol* **12** (2008) 214.
- Ramakrishnan R, and Karunamoorthy L, *J Mater Process Technol* **207** (2008) 343.
- Salehi M, Hosseinzadeh M, and Elyasi M, *Trans Indian Inst Met* (2015). <https://doi.org/10.1007/s12666-015-0670-1>.
- Chockalingam S, Natarajan U, and Kalyana Sundaram S, *Trans Indian Inst Met* (2014). <https://doi.org/10.1007/s12666-015-0707-5>.